Pergamon

Int. J. Heat Mass Transfer. Vol. 39, No. 14, pp. 3079–3082, 1996

0017–9310/96 $15.00+0.00

0017–9310(95)00322–3

Comparison between theoretical models and experimental data for the spreading of liquid droplets impacting a solid surface

W. M. HEALY, J. G. HARTLEY† and S. I. ABDEL-KHALIK

The George W. Woodruff School of Mechanical Engineering, Georgia Institute of Technology, Atlanta, GA 30332-0405, U.S.A.

(*Received* 22 *February* 1995 *and in final form* 25 *August* 1995)

INTRODUCTION

The dynamics of droplet impact are important because of their relevance to a number of engineering applications, e.g. spray cooling, metal forming, ink-jet printing and spray-coating. Of particular interest is evaporative spray cooling, where proper dimensions are needed to predict heat fluxes within the evaporating liquid film formed upon drop impact and to determine proper spacing of drops on the heated surface. Usually macroscopic models, derived from energy conservation, are used to predict the maximum spreading radius of the spreading film. However, the validity of these model assumptions has not been established. Bennett and Poulikakos [1] examined the models of Jones [2], Collings *et al.* [3], Chandra and Avedisian [4] and Madejski [5]. They found that the simplifications made in deriving the first two models made them very inaccurate; hence, those models will not be examined in the present comparison. The models of Chandra and Avedisian [4] and Madejski [5] did show promise and will be included. Four other models have been found that yield expressions for the maximum radius of the film [6–9]. The accuracy of these models is assessed by systematically comparing their predictions with experimental data found in the literature. Since high heat flux spray cooling applications at surface temperatures below the Leidenfrost temperature were of primary interest, this study considers only situations where the drop wets the surface. Five data sets giving the maximum spreading radii of impacting droplets were found [6, 10–13], and four references [4, 13–15] were found which contained data for the transient radius of a spreading film. Table 1 provides a summary of the relevant parameters for those data sets.

DROPLET SPREADING MODELS

In the following discussion, a number of non-dimensional parameters arise. Among these are the spreading ratio, β, the Weber number, We and the Reynolds number of the incoming droplet, Re. The spreading models considered in this study were developed through an energy balance for the impacting droplet. The sum of the initial kinetic and surface energies of the incoming droplet is balanced with the instantaneous kinetic and surface energies of the spreading film and viscous dissipation. Calculating the initial drop energy is a simple matter, but evaluating the energies of the film and viscous dissipation is a more complex problem.

Table 2 summarizes the main features of the six models. Five [4, 5–7, 9] assume that the liquid immediately forms a cylinder upon impact and spreads as an upright cylinder; the sixth model [8] assumes that the droplet deforms as a spherical segment. Models based upon an energy balance between the initial condition and the final, fully-spread liquid film result in an algebraic equation for determining the maximum spreading radius of a drop. Transient energy balance models produce differential equations that predict the time variation of the film radius. The primary difference between the models is the assumed velocity profile within the film (Table 2). In Chandra and Avedisian's model, an order of magnitude analysis was used to estimate the velocity profile. Different methods were used to calculate the viscous dissipation and the surface energy of the spreading film (Table 2). Some models account for the contact angle while others ignore it. In this study a thirty-two degree contact angle was used as suggested in [4], but the results were relatively insensitive to the assumed contact angle.

Equations (1) and (2) present the algebraic models of Kurabayashi–Yang [7] and Chandra and Avedisian [4]. The differential models are not reproduced here because of their complex nature.

$$\frac{We}{2} = \frac{3}{2}\beta_{\max}^2\left[1 + \frac{3We}{Re}\left(\beta_{\max}^2 \ln \beta_{\max} - \frac{\beta_{\max}^2 - 1}{2}\right)\left(\frac{\mu_{\mathrm{drop}}}{\mu_{\mathrm{wall}}}\right)^{0.14}\right] - 6 \quad (1)$$

$$\frac{3We}{2Re}\beta_{\max}^4 + (1-\cos\theta)\beta_{\max}^2 - \left(\frac{We}{3} + 4\right) = 0. \quad (2)$$

RESULTS AND DISCUSSION

Figure 1 shows a comparison between experimental data for the maximum spreading ratio and the predictions of the Kurabayashi–Yang model [7]. Data from all references listed in Table 1 were used. The dashed lines delineate the region in which predictions were within ten percent of the experimental data. Note that the Kurabayashi–Yang model tends to overpredict the spreading ratio. Plots for other models show even greater discrepancies between predicted and experimental values. Percent differences between predicted and experimental values were calculated and are shown in Table 3 along with the standard deviations of the differences. Most of the models tend to overpredict the maximum spreading ratios.

† Author to whom correspondence should be addressed.

NOMENCLATURE

C	constant
d	diameter of spreading film
D	diameter of impacting droplet
$f(r)$	a function of r
h	height of spreading film
r	radial coordinate
Re	Reynolds number $= \rho VD/\mu$
$\mathbf{u}$	velocity in spreading film
V	impact velocity
We	Weber number $= \rho V^2 D/\sigma$
z	axial coordinate.

Greek symbols

β	spreading ratio, d/D
ϕ	dissipation function
μ	fluid viscosity
θ	contact angle between liquid and surface
ρ	fluid density
σ	surface tension
τ	shear stress tensor.

Subscripts

drop	evaluated at droplet temperature
max	maximum
r	radial direction
wall	evaluated at wall temperature
z	axial direction.

Table 1. Parameter ranges for droplet spreading experiments

Reference	Type	Fluid	Surface	D [mm]	V [m s^{-1}]	No. of data points
Ford and Furmidge [10]	M†	Water	Glass, beeswax, cellulose acetate	0.62–1.05	2.61–4.27	15
Toda [11]	M	Water	Glass	2.22–4.70	1.68–5.99	32
Stow and Hadfield [14]	T‡	Water	Buffed aluminum	3.32	2.13	1
Shi and Chen [6]	T,M	Water	Aluminized glass	2.48–4.72	1.02–3.02	T: 9, M: 18
Valenzuela *et al.* [12]	M	Water	Glass	2	0.52–7.05	10
Tsurutani *et al.* [15]	T	Water	?	2.08	0.976	1
Chandra and Avedisian [4]	T	n-Heptane	Stainless steel	1.50	0.93	1
Kurokawa and Toda [13]	T,M	Water, Ethyl Alcohol, Mercury	Glass	1.31–2.31	2.12–4.46	T: 6, M: 6

† M, maximum spreading ratio data.
‡ T, transient spreading ratio data.

Table 2. Droplet spreading models

Model	Model type	Assumed velocity profile	Viscous dissipation	Surface energy
Kurabayashi–Yang [7]	Algebraic	?	?	$\sigma \bullet$ Top surface area of cylinder
Madejski [5]	Differential	$u_z = -Cz^2$; $u_r = Crz$	friction power $= \tau_r^*$ average velocity* area of film bottom	$\sigma \bullet$ Gas–liquid interfacial area
Bechtel *et al.* [8]	Differential	Axisymmetric stagnation point flow	$\tau = C\mu u_r$;	$\sigma \bullet$ Entire surface area of cylindrical film
Shi and Chen [6]	Differential	$u_z = -\frac{2}{3}Cz^3$; $u_r = Crz^2$	$\phi = (\boldsymbol{\tau}:\nabla\mathbf{u})$	Includes contact angle
Chandra and Avedisian [4]	Algebraic	$u_r = O(Vz/\mathrm{h})$	$\phi = (\boldsymbol{\tau}:\nabla\mathbf{u})$	Includes contact angle
Naber [9]	Integro-differential	$u_r = z \cdot f(r)$	$\phi = (\boldsymbol{\tau}:\nabla\mathbf{u})$	Includes contact angle

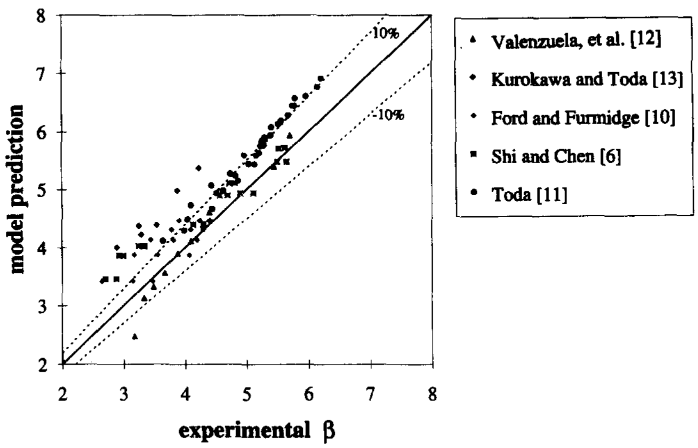

Fig. 1. Example of comparison between predictions of maximum spread and experimental data. Model used in this case is the Kurabayashi–Yang model [7].

Shi and Chen's [6] predictions appear the best, but that conclusion may be misleading since they incorporated an empirical factor in their model. Otherwise, the Kurabayashi–Yang model provides the best predictions with an average deviation of approximately ten percent and a relatively small standard deviation. Other models' predictions deviate significantly from the data. When Naber's model predictions for maximum spreading ratio was divided by a constant factor of 1.37, as suggested in his thesis, excellent predictions resulted as shown in Table 3.

Transient film spreading data were also compared to predictions of the four differential models listed in Table 2. Because the time to reach the maximum radius cannot be exactly determined, the time to reach 95% of the maximum spreading ratio was used in this comparison, and results are shown in Table 3. Although the number of data points used in this comparison is limited, one can see that time predictions deviate significantly from experimental values.

Overall, none of the models adequately predict the dimensions of the spreading film. One problem with these analyses is the assumed shape of the spreading film. The cylindrical and spherical segment assumptions differ significantly from observed spreading shapes. Photographs of an impacting drop [4, 13, 14] show that a thin jet of fluid emerges from the bottom of the drop while the droplet retains its spherical shape well into the impact. Inclusion of the actual shape of the film is not possible, however, until a full solution of the Navier–Stokes equations is known, which is inconsistent with the simplified approach used in these models.

Another area of uncertainty is the treatment of surface effects. Aspects of the surface–liquid interaction, such as the contact angle and surface roughness, were not formally treated in these models although they could have a significant effect on the dynamics of the spreading film. While the work of Stow and Hadfield [14] considered the effect of surface roughness on spreading, none of the models compared here take this factor into account. Some consider the contact angle and others ignore it.

The overpredictions of the models may indicate that they all underestimate viscous losses. The fluid dynamics of the impacting drop are quite complex, so a simple relation for the velocity field may not accurately yield the proper viscous dissipation. Results of Naber [9] and Ford and Furmidge [10] show that viscous dissipation dominates the total energy in the late stages of the spreading process, and underestimating viscous losses could lead to a significant overprediction of the maximum spreading radius.

CONCLUSION

Predictions for the spreading ratio of an impinging droplet have demonstrated much uncertainty in the mechanics of impacting droplets. Theoretical models generally overpredict

Table 3. Differences between predicted and experimental values

	β_{max}†		Time to reach 95% of β_{max}‡	
Model	Mean difference (%)	Standard deviation (%)	Mean difference (%)	Standard deviation (%)
Kurabayashi–Yang [7]	9.9	10.3	N/A	
Madejski [5]	45.6	20.5	59.6	51.2
Bechtel *et al.* [8]	50.5	38.4	6.5	38.8
Shi and Chen [6]§	5.6	16.2	29.4	39.0
Chandra and Avedisian [4]	45.1	14.9	N/A	
Naber [9]	48.5	15.4	50.3	51.8
Corrected Naber [9]‖	8.4	11.3	50.3	51.8

† Data from all references listed in Table 1 were used in this comparison.
‡ Data denoted by "T" (transient spreading ratio data) in Table 1 were used in this comparison.
§ An empirical factor was incorporated in the model of Shi and Chen.
‖ Results of Naber's model were divided by a constant factor of 1.37 as suggested in ref. [9].

the maximum spreading ratios, and predicted times for the spreading process are significantly different from experimental data. The Kurabayashi–Yang equation provided the best estimate for the maximum spreading ratio among the models although it could not be used to predict transient spreading. The majority of the differences between its predictions and experimental values was within 10%. Other models overpredicted the data by approximately 45%.

Acknowledgements—This material is based upon work supported under a National Science Foundation Graduate Research Fellowship to W. M. Healy.

REFERENCES

1. T. Bennett and D. Poulikakos, Splat–quench solidification: estimating the maximum spreading of a droplet impacting a solid surface, *J. Mater. Sci.* **28,** 963–970 (1993).
2. H. Jones, Cooling, freezing and substrate impact of droplets formed by rotary atomization, *J. Phys. D: Appl. Phys.* **4,** 1657–1660 (1971).
3. E. W. Collings, A. J. Markworth, J. K. McCoy and J. H. Saunders, Splat–quench solidification of freely falling liquid-metal drops by impact on a planar substrate, *J. Mater. Sci.* **25,** 3677–3682 (1990).
4. S. Chandra and C. T. Avedisian, On the collision of a droplet with a solid surface, *Proc. R. Soc. Lond. A* **432,** 13–41 (1991).
5. J. Madejski, Solidification of droplets on a cold surface, *Int. J. Heat Mass Transfer* **19,** 1009–1013 (1976).
6. M. H. Shi and John C. Chen, Behavior of a liquid droplet impinging on a solid surface, Presented at 1983 ASME Winter Annual Meeting. Preprint no. 83-WA/HT/104 (1983).
7. W. J. Yang, Theory on vaporization and combustion of liquid drops of pure substances and binary mixtures on heated surfaces, 535, Institute of Space and Aeronautical Science, University of Tokyo, Tokyo (1975).
8. S. E. Bechtel, D. B. Bogy and F. E. Talke, Impact of a liquid drop against a flat surface, *IBM J. Res. Development* **25,** 963–971 (1981).
9. J. D. Naber, Droplet impingement on a heated surface, Ph.D. Thesis, University of Wisconsin, Madison, Wisconsin (1992).
10. R. E. Ford and C. G. L. Furmidge, Impact and spreading of spray drops on foliar surfaces. In *Wetting: A Discussion Covering both Fundamental and Applied Aspects of the Subject of Wetting and Wettability*. Society of Chemical Industry, London, (1967).
11. S. Toda, A study of mist cooling (2nd report: theory of mist cooling and its fundamental experiments), *Heat Transfer-Jap. Res.* **3,** 1–44 (1974).
12. J. A. Valenzuela, T. J. Jasinski and B. C. Drew, High heat flux evaporative cold plate for space applications, TM-1103, Creare Inc., Hanover, New Hampshire, Phase I Final Report, NASA Contract NAS9-17574 (1986).
13. M. Kurokawa and S. Toda, Heat transfer of an impacted single droplet on the wall, *ASME/JSME Thermal Engng Proc.* **2,** 141–146 (1991).
14. C. D. Stow and M. G. Hadfield, An experimental investigation of fluid flow resulting from the impact of a water drop with an unyielding dry surface, *Proc. R. Soc. Lond. A* **373,** 419–441 (1981).
15. K. Tsurutani, M. Yao, J. Senda and H. Fujimoto, Numerical analysis of the deformation process of a droplet impinging upon a wall, *JSME Int. J.* **33,** 555–561 (1990).